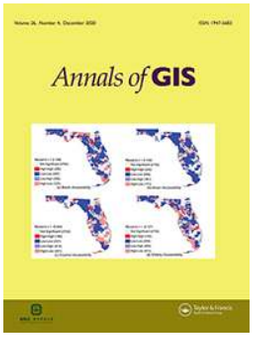

Annals of GIS

ISSN: (Print) (Online) Journal homepage: https://www.tandfonline.com/loi/tagi20

Land use/land cover and land surface temperature analysis in Wayanad district, India, using satellite imagery

Jovish John, G. Bindu, B. Srimuruganandam, Abhinav Wadhwa & Poornima Rajan

To cite this article: Jovish John, G. Bindu, B. Srimuruganandam, Abhinav Wadhwa & Poornima Rajan (2020) Land use/land cover and land surface temperature analysis in Wayanad district, India, using satellite imagery, Annals of GIS, 26:4, 343-360, DOI: 10.1080/19475683.2020.1733662

To link to this article: https://doi.org/10.1080/19475683.2020.1733662

Published online: 02 Mar 2020.

ANNALS OF GIS
2020, VOL. 26, NO. 4, 343–360
https://doi.org/10.1080/19475683.2020.1733662

Taylor & Francis
Taylor & Francis Group

Land use/land cover and land surface temperature analysis in Wayanad district, India, using satellite imagery

Jovish John[a], G. Bindu[b], B. Srimuruganandam[a], Abhinav Wadhwa[c] and Poornima Rajan[b]

[a]School of Civil Engineering, Vellore Institute of Technology, Vellore, India; [b]Nansen Environmental Research Center (India), Kochi, India; [c]Centre for Disaster Mitigation and Management, Vellore Institute of Technology, Vellore, India

ABSTRACT

This paper assesses Land Use/Land Cover (LULC) classification and Land Surface Temperature (LST) in Wayanad district during the years 2004 and 2018. The LULC classification of Wayanad district is identified using IRS P6 (Linear Imaging Self Scanner) LISS- III, and LST using thermal band of (Enhanced Thematic Mapper Plus) ETM+ imageries. Maximum likelihood classification (MLC) technique is opted to categorize six land-use features: water body, paddy field, forest, dense, agricultural crops and built-up. From 2004 to 2018, impacts of changes in features are correlated with the raised LST. Overall vegetation cover shows an increasing pattern during the study period. The water bodies in Wayanad district improved from 4.30 to 32.68 sq.km due to construction of two dams: Banasurasagar and Karappuzha. However, agricultural crops and paddy field area have decreased by 4.7% in last 14 years. Decreasing rate of agricultural crops can be directly linked to population growth, thereby developing various built-up zones for basic needs. Forest and dense vegetated cover area are increased nearly 2.3 and 3.0%, respectively, during the study period, while bamboo degradation has also been witnessed from 2008 to 2013. The built-up class shows growth from 1.48 to 5.69% of total land area during 2004 and 2018. LULC have noticeable influences on LST with a negative correlation between vegetation cover and LST with a decrease of 1.75°C. The study findings can help the local authorities to implement urban planning regulations for public awareness and policy makers for a sustainable planning and management in forthcoming years.

ARTICLE HISTORY
Received 22 July 2019
Accepted 18 February 2020

KEYWORDS
Land use/land cover; land surface temperature; vegetation indices; GIS and remote sensing

1. Introduction

1.1 General

LULC changes mapping and its impacts at regional scales serve a wide range objective to mitigate and manage various disasters like landslides, global warming, urban flooding, etc., (Reis 2008). The change-detection study negatively affects the climatic patterns, hazard susceptibility, biodiversity loss, global and local socio-economic dynamics (Mas et al. 2004; Dwivedi, Sreenivas, and Ramana 2005; Zhao, Lin, and Warner 2004). Rapid conversion of various land covers to different land use patterns is observed globally (Lambin, Geist, and Lepers 2003). Land-cover variations mainly depend on population growth of an area along with human intervention (Achmad et al. 2015), agricultural demands (Cammerer, Thieken, and Verburg 2013; Li, Zhou, and Ouyang 2013; Dale et al. 1997), natural calamities (Dubovyk, Sliuzas, and Flacke 2011), economic and urbanization development (Rimal et al. 2019; Khan et al. 2014), and other factors (Mustafa et al. 2018). With realization that global environment is strongly influenced by land surface, concerns about LULC emerged in research areas. Availability of land-use change statistics aids in the decision-making process for environmental planning and management (Prenzel 2004; Fan, Weng, and Wang 2007). Land cover conversion modifes surface-albedo, which in turn increases energy exchanges between atmosphere and surface thus introducing an impact on local climate (Sagan, Toon, and Pollack 1979). Metropolises with diverse physical surfaces than the surrounding rural areas show impact on their microclimate (Cai, Du, and Xue 2011). There are numerous developmental activities and policy implementations by government revolving around the changes in urban development resulting into forest loss of nearly 40% over India during 1880 and 1980 (Flint 1994).

Only a few studies are conducted on some Indian metropolitan cities like Delhi (Mallick, Kant, and Bharath 2008), Jaipur (Jalan and Sharma 2014) and Chennai (Amirtham and Devadas 2009), but fewer research works are carried out in Wayanad district of Kerala on this aspect. From 2008 onwards, a large-scale degradation of bamboo plantation has occurred in Wayanad district thus growing concerns in forest department. To keep the vulnerability of landslides (Kuriakose, Sankar, and Muraleedharan 2009) and increased migration of permanent residents to

CONTACT B. Srimuruganandam bsrimuruganandam@vit.ac.in School of Civil Engineering, Vellore Institute of Technology, Vellore 632014, India

Wayanad district, the present study of land-cover change detection is engrossed at this juncture.

Global coverage of Land Surface Temperature (LST) can be derived from series of satellites like Landsat, Terra and Aqua with higher spatial resolutions (Zhu, Lu, and Jia 2013). The transformation of vegetated areas to build up (Mallick, Kant, and Bharath 2008) and conversion of wetland and marshland into agricultural cultivation land or bare waste land (Pal and Akoma 2009) plays vigorous role in LST increase. The other causative factors responsible for urbanization increase in correlation with climate change (Mustafa et al. 2018). The author cited a vibrant investigation of factors like topography of the area, zoning status, population density, employment opportunities, Euclidean distance from national and state highways, railways, commercial areas, religious monuments, etc., responsible to increase in urban sprawl. A hybrid model is used to predict LULC by combining logistic reasoning and cellular automata growth models for Ahmedabad city and concluded that the population increase contributes maximum to the LULC changes because of extra land-living parcel requirement (Mustafa et al. 2018). Also, an investigation on allocation of different built-up classes for the study area simplifies the study of the aforementioned factors' influence on various climatic factors like temperature, rainfall, air pollution, etc. (Verma et al. 2016; Rollet et al. 1998; Schneider 2012; Mohan et al. 2012; Loibl and Toetzer 2003). Study of the relation between LST and LULC changes helps to solve problems related to climatic change and analyse interactions between human and environment (Jha, Dutt, and Bawa 2000). LST values of all pixels with their thermal reflectance have correlation with neighbourhood pixel DN values (Song et al. 2014). Modelling current surface temperatures with respect to LULC plays a vital role in mitigating rapid climatic change. New policies and guidelines in urban or rural land-use planning can be adopted for reducing heating effect based on the results.

Remote sensing is proved to be a very useful advanced tool for LULC variation detection. Remotely sensed data and Geographical Information Systems (GIS) are considered as one of the effective responsive tools for urban climate studies (Deep and Saklani 2014). The use of satellite imageries creates lenience to fetch ground truth data of protected zones as well as tough terrains like Wayanad, India. The necessity of spatial data to obtain LST and LULC is driving investigators to identify pertinent satellite-based approach, which will overcome the above-said difficulties in surveying remote locations. Remotely sensed data has become one of significant applications for mapping change in LULC with varied applications (Lo and Choi 2004). This study for change detection is mainly aimed to assess the change that occurred in LULC in Wayanad district during 2004 and 2018, and establish its correlation with LST. The LULC map and LST map are developed and observed using Linear Imaging Self Scanner (LISS) III and Enhanced Thematic Mapper Plus (ETM+), respectively. The correlation of individual land-use features with LST change is also analysed in this study.

2. Materials and methods

2.1 Site description

Study area (as shown in Figure 1) is selected as Wayanad district (11°44′ N–11°97′ N and 75°77′ E–76°43′ E), located in North-Eastern region of Kerala, India. The altitude of study area varies from 700 to 2100 m above mean sea level on the crest of the Western Ghats and covers an area of 2130 sq.km. As the Western Ghats is a part of UNESCO's world heritage site and world's biodiversity hotspot, a diverse range of flora and fauna can be observed in this green paradise. Nearly 40% of the total land area of district is under forest-protected zone (Sand 2016). The backbone of district's economy is mainly based on agriculture. Wayanad is famous for its rice and pepper production and the other agricultural crops produced in the district are coffee, tea, coconut, plantain and cardamom.

The increased population and landslides in this high range causes a large LULC variation in the stud area. A large area of the district is under forest-protected zone. About 25.6% forest cover loss is observed between 1973 and 1995 in the southern parts of the Western Ghats (Jha, Dutt, and Bawa 2000). Wayanad district is the only district of Kerala sharing boarder together with Karnataka (north and north-east direction) and Tamil Nadu (south-east direction) states of India. The annual mean rainfall of the district is 2322 mm and average temperature for last 5 years ranges from 18 to 29°C. The population of the Wayanad district is 8,17,420 with assorted locales of the two adjoining states (Sand 2016). The granite quarries in various parts of the districts convert most of the ecologically sensitive areas into landslide-prone areas. Usual landslide activities (Kuriakose, Sankar, and Muraleedharan 2009) often result in land change in the region. Rapid urban developmental activities, vast degradation of bamboo plantations and annual variation of weather conditions in the district are motivations to select the study area.

2.2 Satellite data used

In this study, remotely sensed satellite imageries are used for the LULC classification and the LST estimation of

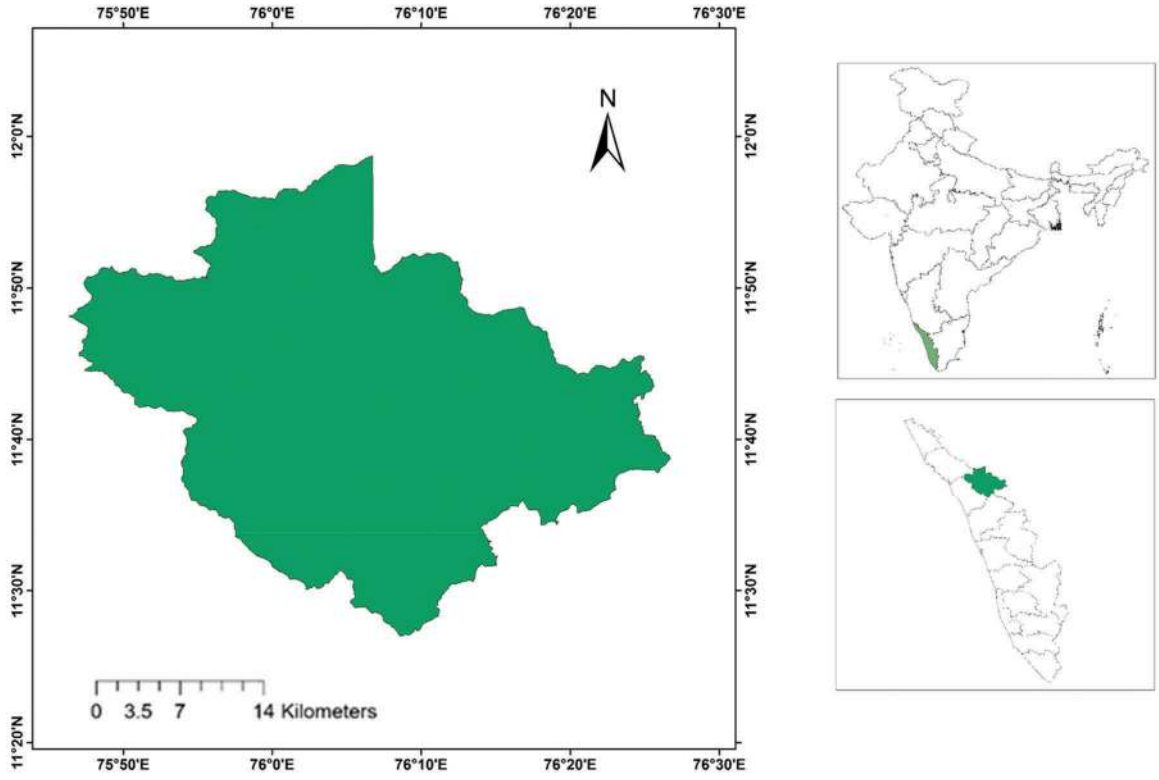

Figure 1. Location map of study area (Wayanad).

Wayanad district during the years 2004 and 2018. Multispectral satellite imageries of LISS III sensor and ETM+ sensor fetched datasets during 2004 and 2018 are used for this study. LISS III sensor carried on RESOURCESAT-1 (formerly known as IRS-P6) and RESOURCESAT-2A of Indian Space Research Organization (ISRO) with a spatial resolution 23.5 m is used for LULC classification of 2004 and 2018, respectively. Whereas satellite imageries of ETM+ Land Remote Sensing Satellite (Landsat-7) of National Aeronautics and Space Administration (NASA), United States, with a spatial resolution 30.0 m is used for the LST estimation in the study area during 2004 and 2018. In this study, three bands of LISS-III Green (Band 2), Red (Band 3) and Near Infrared (Band 4) are used for LULC classification and Thermal band (Band 6) of ETM+ is used for LST estimation. LISS-III satellite imageries used for LULC classification are purchased from National Remote Sensing Centre (NRSC), Hyderabad, and ETM+ imageries used for LST analysis are freely downloaded from the United States Geological Survey (USGS) website. The detailed description of datasets used in this study is presented in Table 1.

The origin of the study and selection of period of comparison is chosen to address two major aspects of land-use changes and its impacts on rising temperature in Wayanad district. Firstly, a pre-developed cloud free coherent satellite image is obtained to produce LULC map of specific study area that can be used as a benchmark digital data in future for LULC variation analysis. Next, cloud-free satellites images are essential for LULC mapping and LST analysis after necessary radiometric and geometric corrections. The presence of atmospheric clouds acts as barrier for satellite's image capturing payload. After considering all conditions, the satellite imageries from LISS-III sensor acquired on February 2004 and January 2018 for LULC mapping are obtained in tiff format. ETM+ imageries of January 2004 and 2018

Table 1. Sensor specifications of LISS-III and ETM+ imageries used.

Satellite/Sensor	Date of Pass	Path/Row	Source
ResourceSat-1/LISS – III	14.02.2004	099/065	National Remote Sensing Agency (NRSC), India
ResourceSat-2A/LISS – III	19.01.2018	099/065	(https://bhuvan.nrsc.gov.in/bhuvan_links.php)
Landsat 7/ETM+	14.01.2004	145/052	United States Geological Survey (USGS), United Sates
Landsat 7/ETM+	24.02.2004	144/052	(https://earthexplorer.usgs.gov)
Landsat 7/ETM+	20.01.2018	145/052	
Landsat 7/ETM+	29.01.2018	144/052	

are used for LST estimation. A preparatory version of ArcGIS 10.1 and Envisat is used for pre-processing the satellite images and Figure 2 shows a detailed methodology used in this study.

2.3 Image pre-processing

Satellite imageries are necessary to pre-process for more accurate and precise information. Initially, the satellite images obtained are geometrically corrected for LISS-III images using UTM coordinate system and radiometrically corrected for ETM+ images as a part of standard pre-processing procedure. The geometric correction can be achieved by choosing accurate Ground Control Points (GCP) on satellite imagery and on suitable geometric model (Thakkar et al. 2017). Georeferenced Landsat 7 ETM + images acquired from USGS Earth Explorer website after 31 May 2003 have traces of zig-zag lines over satellite ground path. This error is occurred due to failure occurred to malfunction of Scan Line Corrector (SLC): ETM+ sensor. Therefore, radiometric correction is performed on ETM+ (SLC failed) images to make it more useful. Radiometric correction is performed using Landsat toolbox developed for ArcGIS 10.1 (Foody 2002) to correct distortions occurred in ETM+ satellite imageries.

To classify the satellite images, supervised and unsupervised learning techniques have adopted grounded based on intricacy involved in the image classification . Review study on the image classification techniques presents all types of classification techniques and their inferences once equated to the validation dataset (Li et al. 2014). There are seven types (Maximum Likelihood Classifier, MLC) (Settle and Briggs 1987; Shalaby and Tateishi 2007), Naive Bayes Classifier (Minimum Distance-to-Means Classifier) (Atkinson and Lewis 2000), Mahalanobis Distance Classifier (Deer and Eklund 2003), Neural Networks (Kavzoglu and Mather 2003) Support Vector Machines (SVM) (Huang, Davis, and Townshend 2002; Pal and Mather 2005; Marconcini, Camps-Valls, and Bruzzone 2009), Decision Trees (McIver and Friedl 2002; Jiang et al. 2012), Boosted Trees (Friedl and Brodley 1997), Random Forest (Gislason, Benediktsson, and Sveinsson 2006)) of supervised and two types (k-means (Rollet et al. 1998; Blanzieri and Melgani 2008) and ISO-data (Dhodhi et al. 1999) of unsupervised techniques available in Envisat and are most extensively used techniques. Unsupervised classification techniques work on pixel-based analysis in which pixels are grouped into families as defined by the user in the number of classes (minimum and maximum classes in case of ISO-data technique). K-means algorithm works on the principle of finding the scalar Euclidean distance between pixels and merging them into classes either as maximum iterative classes with minimal error or as defined by the operator (whichever is smaller). In supervised learning-based algorithms, the training datasets are selected in the order of 10 *n* (where *n* is the number of bands selected for image

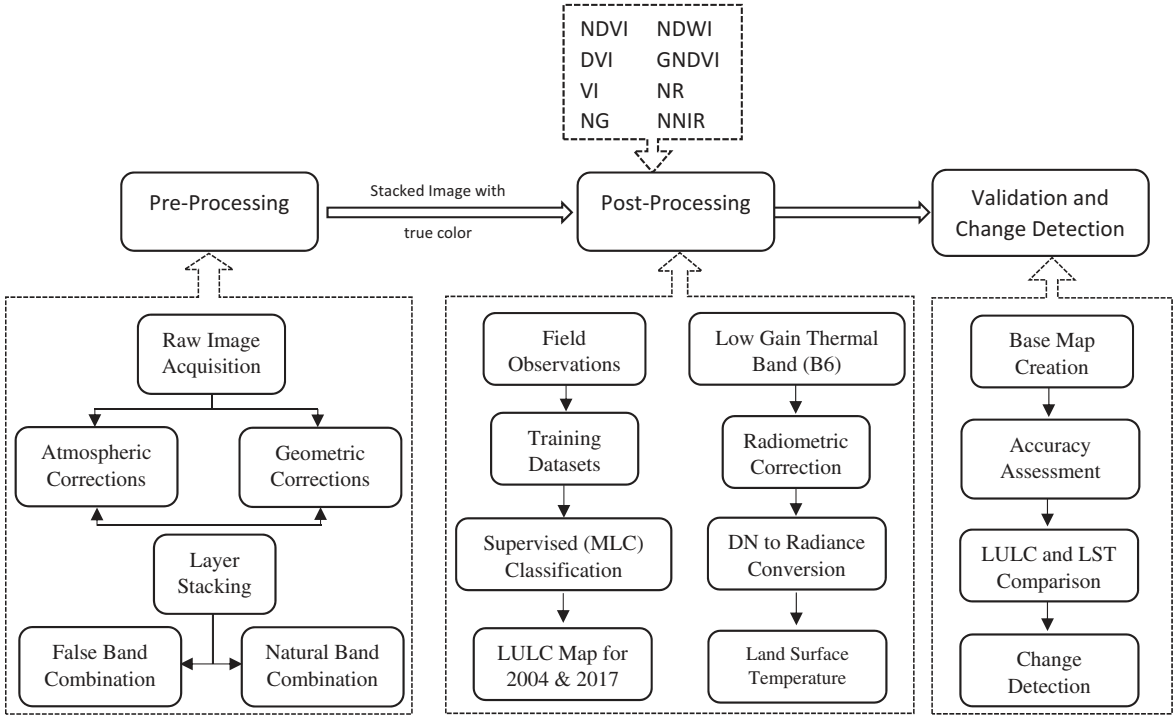

Figure 2. LULC and LST methodology.

classification). According to the review of literature on above-mentioned supervised technique, the MLC is chosen as the most effective classification technique (after image enhancement using principal component analysis) (Li et al. 2014).

2.4 Training dataset

In general, supervised and unsupervised classification techniques are adopted to classify various features in the area and determine their land characteristics. In the present study, we are applying the MLC (supervised classification) technique for better LULC mapping. Extraction of training data is one of the critical and time-consuming activities in the supervised classification process. Training sample point selection for any supervised classification technique is helpful in estimating mean vector and co-variance matrix aiding to calculate discriminant function for individual feature. The quantity and quality of input training dataset is the principal factor that primarily increases LULC accuracy level, i.e. higher the number and quality of training samples, higher will be the accuracy of LULC classification. So, training pixels of six classes are designated from the regions after inspecting reference map and post-field surveys. The characteristics of false colour image (obtained using various band combinations) for LULC classification is given in Table 2. The total number of training pixels must be higher enough for better and accurate LULC classification. Number of input training pixels for each classification must be kept minimum 30 times the total number of bands used for the study (Mather and Koch 2010). The MLC technique is adopted to classify six land-use classes by taking a minimum of 100 sample training points for each feature class (Schneider 2012).

2.5 LULC accuracy assessment

For the accuracy assessment, the classified results are compared with available reference datasets, which is assumed to be correct for defining a classification. Several methods are adopted to analyse user and overall accuracy of remote-sensed data (Aronica and Lanza 2005). LULC change accuracy is influenced by factors like sensor component associated issues and data pre-processing methods used with standard conditions at the image acquisition time (Morisette and Khorram 2000). In this study, we are using error matrix or confusion matrix technique (Foody 2002) for post-classification comparison method. Agreement and disagreement of pixels are generally compiled in the error matrix method. The rows of the error matrix table represent the reference data while the columns represent classified data (Morisette and Khorram 2000). For 2004 and 2018, the numbers of sampling points for post-classification validation of the six classes are 319 and 297, respectively, and using Equation 1, the percentage overall accuracy of each feature is calculated.

$$Overall\ Accuracy = \frac{Total\ Number\ of\ Correct\ pixels}{Total\ Number\ of\ Pixels} * 100 \quad (1)$$

2.6 Land surface temperature analysis

All the satellite imageries comprise of pixel arrays that contain intensity value and location address which are digitalized and stored in the form of Digital Number (DN). The DNs are processed to convert into temperature scale using Equation 2. Image pixels are converted from DNs are rescaled to spectral radiance by using radiometric rescaling coefficient and are further converted to brightness temperature using thermal constants. When digital data are used for analysis, conversion of raw DNs to equivalent radiance or reflectance value for the comparison with other datasets is necessary (McFeeters 1996). The formulas used for conversion process are given below.

2.5.1 Conversion to radiance

The Scan Line Corrected (SLC) low-gain thermal band of ETM+ image is primarily converted from DN back to radiance scale (USGS LANDSAT 7 (L7) DATA USERS HANDBOOK Version 1.0 2018) using Equation (2).

Table 2. Characteristics of LULC classification of LISS-III data with false colour combination.

Land cover classes	Description	Characteristics on LISS-III data
Water bodies	Reservoirs, rivers and lakes	Blue to deep blue according to depth of water
Paddy field	Paddy field/Rocky outcrops	Lemon yellow
Forest	Wild life Sanctuaries/Protected zones	Apple/Peacock green
Dense vegetation	Tall trees and dense vegetation	Dark green rough texture
Agricultural land	Farm land/crop land	Dark ecru
Built-up	Towns, buildings, roads and other manmade structures	Vermillion red

$$L\lambda = \left(\frac{LMAX\lambda - LMIN\lambda}{QCALMAX - QCALMIN}\right)(QCAL - QCALMIN) + LMIN\lambda \quad (2)$$

Where,

$L\lambda$ = Spectral radiance at aperture of sensor (Watts/(m^2*sr*μm))

$LMAX\lambda$ = Spectral radiance scaled to QCALMAX (Watts/(m^2*sr*μm))

$LMIN\lambda$ = Spectral radiance scaled to QCALMIN (Watts/(m^2*sr*μm))

$QCALMAX$ = Maximum quantized calibrated pixel value in DN = 255

$QCALMIN$ = Minimum quantized calibrated pixel value in DN = 0

$QCAL$ = Quantized calibrated pixel value in DN (varies each pixel & image)

2.5.2 Conversion to temperature from radiance

In the next process, converted spectral radiance of thermal band of ETM+ sensor is further processed to temperature in Kelvin (K) scale using below Equation (3).

$$T = \frac{K2}{\ln\left(\frac{K1}{L} + 1\right)} \quad (3)$$

Where, T = Effective satellite temperature (K)

$K2$ = Thermal band calibration constant two

$K1$ = Thermal band calibration constant one

Further, converted temperature scale in K of thermal band can be again transformed into degree Celsius (°C) using below Equation (4).

$$T(^{\circ}C) = T - 237.15 \quad (4)$$

2.7 Normalized vegetation indexes

Different vegetation indices are developed by combination of green (Band 2), red (Band 3) and near-infrared (Band 4) spectral bands of LISS-III sensor. Eight vegetation indices namely Normalized Difference in Vegetation Index (NDVI) (Zhu, Lu, and Jia 2013), Normalized Difference in Water Index (NDWI) (McFeeters 1996), Green Normalized Difference in Vegetation Index (GNDVI) (Buschmann and Nagel 1993), Vegetation Index Green (VI green) (Gitelson et al. 2002), Normalized Red (NR), Normalized Green (NG) and Normalized Near-infrared (NNIR) (Sripada et al. 2006) are developed using combinations of three spectral bands of LISS-III imagery of 2004 and 2018 (Verma et al. 2016). The equations used for estimation of various vegetation indices are given below:

$$NDVI = \frac{\rho nir - \rho red}{\rho nir + \rho red} \quad (5)$$

$$MNDWI = \frac{\rho green - \rho nir}{\rho green + \rho ni} \quad (6)$$

$$DVI = \rho nir - \rho red \quad (7)$$

$$GNDVI = \frac{\rho nir - \rho green}{\rho nir + \rho green} \quad (8)$$

$$VIgreen = \frac{\rho green - \rho red}{\rho green + \rho red} \quad (9)$$

$$NR = \frac{\rho red}{\rho green + \rho red + \rho nir} \quad (10)$$

$$NG = \frac{\rho geen}{\rho green + \rho red + \rho nir} \quad (11)$$

$$NNIR = \frac{\rho nir}{\rho green + \rho red + \rho nir} \quad (12)$$

3. Results

3.1 Land Use/Land Cover (LULC) classification

Usually, LULC classes are chosen and fixed as per the requirements of specific study and application. In this study, we have classified the area into six LULC classes. Anderson's standard classification system (Anderson et al. 2017) is used for LULC classification. The six LULC classifications used in this study are Water body, Paddy field, Agricultural crop land, Forest, Dense and Built-up area. The detailed description of these classes along the characteristics of LISS-III data with False Colour Composite (FCC) is provided in Table 2. The Wayanad district in Kerala, India, is reported to be facing serious environmental issues like landslides (Antherjanam, Chandrakaran, and Adarsh 2010) and bamboo degradation caused due to rapid LULC variation as a result of population growth and human interventions. Water body class indicate the reservoirs, rivers, lakes and ponds in the study area. The shadows of mountains are misclassified and fused under water body due to identical pixel values. Paddy field classification characterizes not only cultivatable paddy field, but also rocky outcrops, fallow lands, barren lands and open grounds falls under this class. Next classification describes the cash crops, food crops cultivating areas as well as trees in private lands falls under agricultural crop land class. Some dense cover existing in hilly terrain with similar pixel values of agricultural crop lands also belongs to same agricultural crop land class. Wildlife sanctuaries and protected zones are described under forest class. Some aged trees in agricultural areas are also

miscategorized in forest class due to identical pixel values. The thicker and denser vegetative areas especially protected zones in the district are classified as dense vegetated class. Further, some agricultural crop land areas with thick vegetation also fall under dense vegetated classification. Finally, the built-up areas are primarily urban and rural settlements, stone mining areas and roadways in study area are categorized under this. All the six classification are mentioned in Table 2.

3.1.1 LULC accuracy assessment

Various accuracy measures like overall accuracy, user's accuracy, producer's accuracy (Russell and Congalton 2013) and Cohen's Kappa coefficient (Fleiss, Cohen, and Everitt 1969) are calculated for the present study. Overall accuracy indicates the accuracy of whole LULC classification, whereas user's accuracy and producer's accuracy specify accuracy of individual classification. The Cohen's kappa coefficient shows the chances of agreement in a classified data. In this study, two error matrix tables are generated for the final LULC classification. The LULC classification shows an overall accuracy of 81.19 and 76.09% during 2004 and 2018, respectively. User's accuracy and producer's accuracy are obtained from error matrix table of both 2004 and 2018 as shown in Tables 3 and 4. During 2004 and 2018, the Cohen's Kappa coefficient shows 0.74 and 0.67, respectively. The Cohen's Kappa coefficient shows a good agreement as the values falls between 0.61 and 0.80 (Mather and Koch 2010).

3.1.2 Changes in LULC

The changes in LULC of Wayanad district during 2004 and 2018 are shown in Figures 3 and 4. Overall, the whole study area shows an increasing pattern of vegetation cover in LULC map from 2004 to 2018. In 2004, water body exists only 0.2% of district's total land area (2130 sq.km), which increased up to 1.53% later in 2018. The main reason for water body area increase is due to the commissioning of two dams namely Banasurasagar dam and Karappuzha dam during the mid of 2004. So, the reservoirs' image is captured only on satellite imagery of 2018. Increasing trend of water class due to dams commissioned in the area can prove helpful to facilitate daily water requirement for the increasing population. Degradation of thick vegetation particularly bamboo near rivers makes water body pixels more visible for the satellite imagery of 2018 rather than 2004. The shadows of large mountains are also misclassified under water bodies.

From 2004 to 2018, the paddy field area is reduced from 352.32 to 219.01 sq.km, i.e. a loss of nearly 6.26% paddy cultivation area is observed. Currently, paddy cultivation is not at all profitable due to higher labour cost and low market rates. So, farmers are pushed to convert paddy field into other cash crops and food crops like banana, tapioca, ginger and yam cultivating areas.

Table 3. Accuracy assessment of LULC classification of 2004 using error matrix.

	Water body	Paddy field	Forest	Dense	Built-up	Agricultural	Total	Com	User's accuracy
Water body	**1**	0	1	0	0	0	2	0.5	50.0000
Paddy field	0	**36**	4	3	1	7	51	0.29	70.5882
Forest	0	0	**85**	0	0	16	101	0.15	84.1584
Dense	0	0	0	**33**	0	3	36	0.08	91.6666
Built-up	0	2	1	0	**16**	0	19	0.15	84.2105
Agricultural crops	0	0	12	10	0	**88**	110	0.2	80
Total	1	38	103	46	17	114	319	Overall Accuracy 81.191	
Err Omi	0	0.05	0.17	0.28	0.05	0.22		Cohen's Kappa 0.744	
Producer's Accuracy	100	94.7368	82.5242	71.7391	94.1176	77.1929			

Table 4. Accuracy assessment of LULC classification of 2018 using error matrix.

Classification	Water body	Paddy field	Forest	Dense	Built-up	Agricultural	Total	Err Com	User's accuracy
Water body	**4**	0	0	1	0	0	5	0.2	80
Paddy field	0	**28**	2	1	1	9	41	0.317073	68.2926
Forest	0	1	**78**	0	0	25	104	0.25	75
Dense	0	1	0	**31**	0	5	37	0.162162	83.7837
Built-up	0	3	0	0	**14**	0	17	0.176471	82.3529
Agricultural crops	0	4	5	10	3	**71**	93	0.236559	76.3440
Total	4	37	85	43	18	110	297	Overall Accuracy 76.094	
Err Omi	0	0.2432	0.0823	0.2790	0.2222	0.3545		Cohen's Kappa 0.679	
Producer's accuracy	100	75.6756	91.7647	72.0930	77.7777	64.5454			

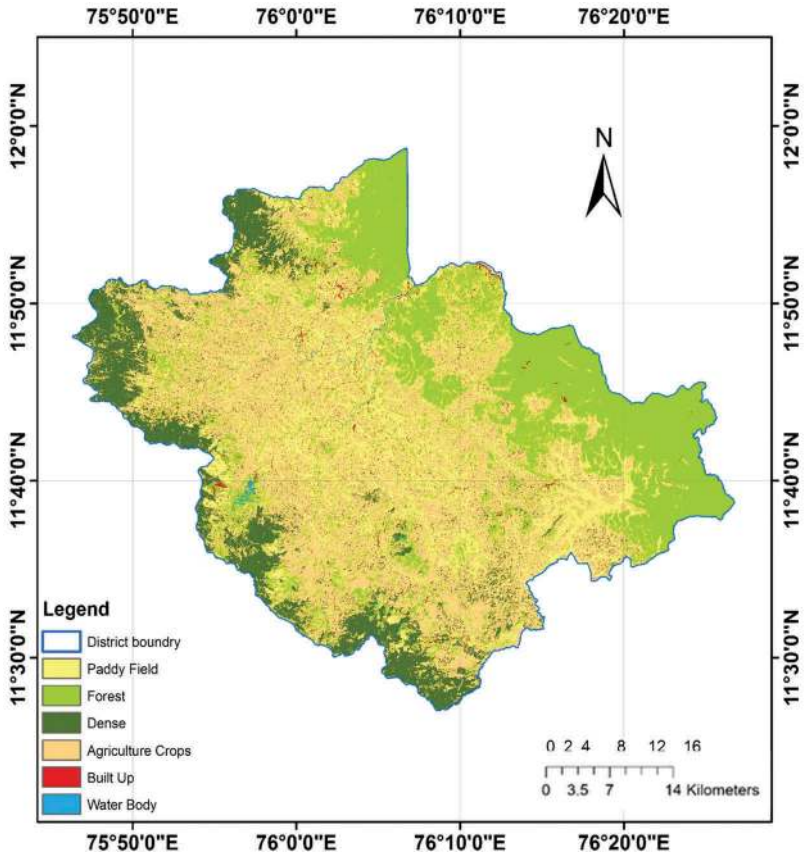

Figure 3. LULC classification of Wayanad 2004.

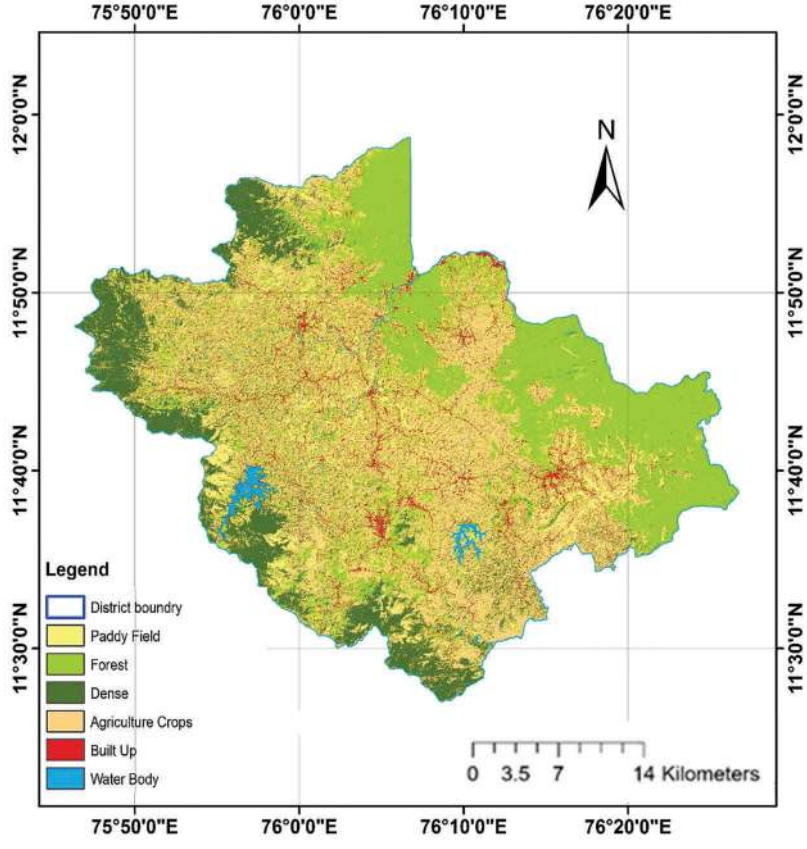

Figure 4. LULC classification of Wayanad 2018.

During the site visit, we also observed ground water depletion in open wells near paddy field which are now converted into other agricultural crops land. Fallow paddy field can have a negative effect on ground water level (Anderson et al. 2017). Paddy fields near to roadsides are nowadays converted into built-up areas for economic benefits.

Mostly, agricultural crops are transforming into built-ups due to increase in population. According to census data, 817,420 people reside in the study area and have 190,894 households (Nagar and Kawdiar 2018). Agricultural crop land areas are also decreased nearly 4.7% within 14 years, i.e. from 865.22 to 764.40 sq.km. Some agricultural crop lands are mainly cleared for cash crops like yam and ginger. Few agricultural crop land areas are misclassified under forest class due to the aged trees in agricultural cultivating lands, as a reason of which pixels show similar values of forest and dense class.

Better growth of vegetation is observed for forest and dense vegetated LULC classes between 2004 and 2018. There is an overall increase from 620.63 to 672.01 sq.km in forest class. Dense vegetated class shows an increase from 12 to 15% (255.56–320.26 sq.km). The strict rules and regulations are followed by government for recent years against human activities in protected areas. At present, both forest and dense LULC classes are not disturbed by human to certain extend; hence, the vegetation in those classes shows slight increase. The increase in forest area helps to restrict the urban development and provides additional benefits to restore the ecology of the area.

A dramatic increase of built-up class is experienced in the study area between 2004 and 2018. The built-up area is increased from 31.55 to 121.21 sq.km during the study period, i.e. an increase of 5.29% in 2018. Population increase is one of the driving factors for drastic growth in built-up area. The rocky areas are also classified under built-up class due to similar pixel values with normal built-up area. The operation of stone mining activities at various location of study area also increased the built-up class area. Approximately, 55 stone mining activities are working till 2016 (Nagar and Kawdiar 2018). The rural built-ups are growing well rather than urban built-ups in the study area. On analysing resultant LULC maps of both years, most of the roadways are mapped better in LULC map of 2018 due to clearance of vegetation near the roadways and wider road than 2004. The variation of LULC classes during 2004 and 2018 is illustrated in the Figure 5.

3.1.3 Vegetation indices

The NDVI enhances all vegetation and tends to have positive value. Soil may exhibit nearby zero value, and all water body features have negative values (McFeeters 1996). Only red band and NIR band of LISS-III images are used for NDVI analysis. In 2004, NDVI values ranges from −0.365079 to +0.763158; whereas for NDVI values during 2018, it ranges from −0.322581 to 0.875862, which means the vegetation cover has increased in 2018 when compared to 2004 in Wayanad district (Figures 6 and 7).

The NDWI is identified to monitor the presence of water bodies. NDWI is used to recheck the increase of water body area during 2004 and 2018. Like NDVI, water index scale also ranges from −1 to +1. The NDWI scale shows −0.4740 to +0.6266 and −0.7288 to +0.5312 during 2004 and 2018, respectively (Figures 8 and 9). The

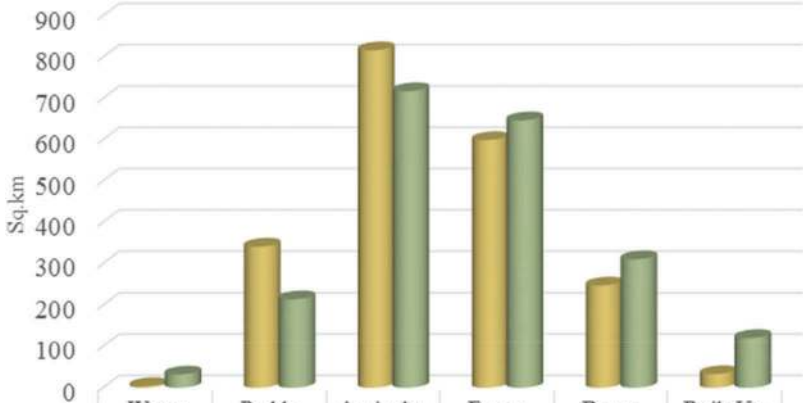

	Water Body	Paddy Field	Agricultural Land	Forest	Dense	Built Up
2004	4.17	341.16	816.65	599.16	247.69	33.06
2018	32.21	214.43	717.55	646.83	310.45	120.52

Figure 5. LULC change analysis in Wayanad during 2004 and 2018.

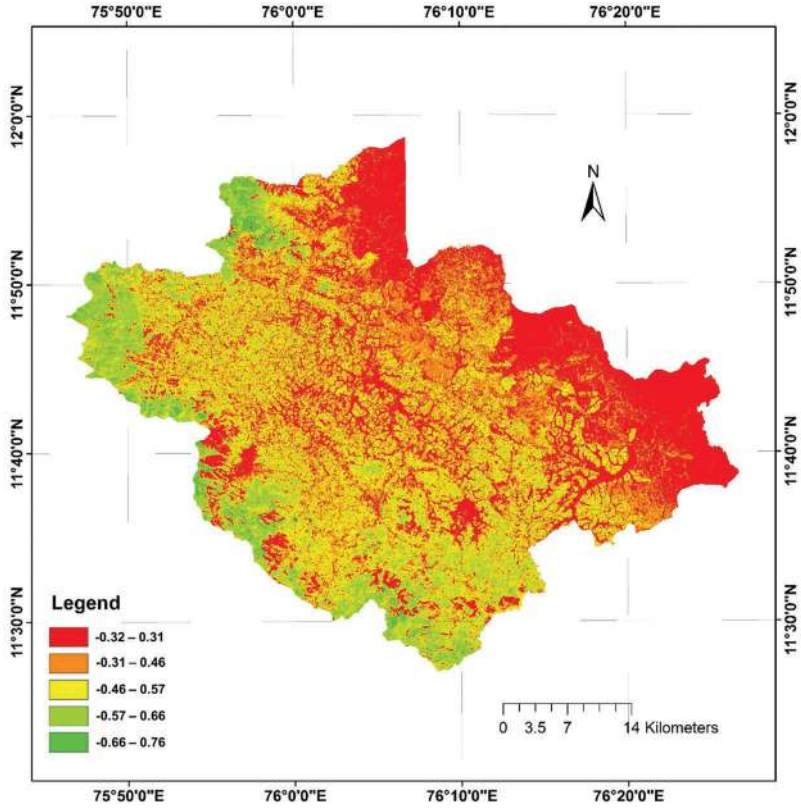

Figure 6. NDVI 2004.

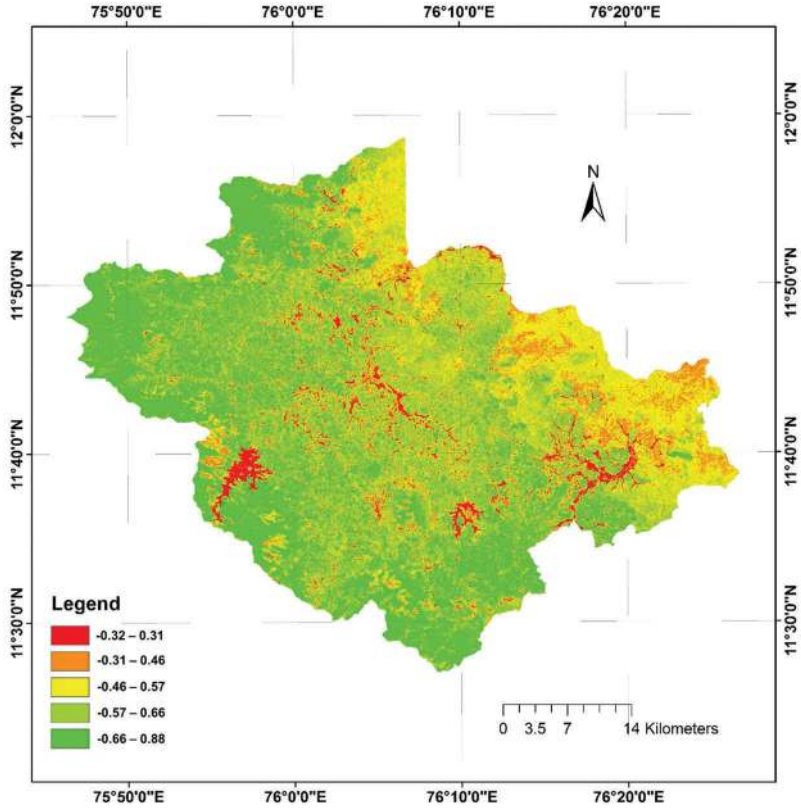

Figure 7. NDVI 2018.

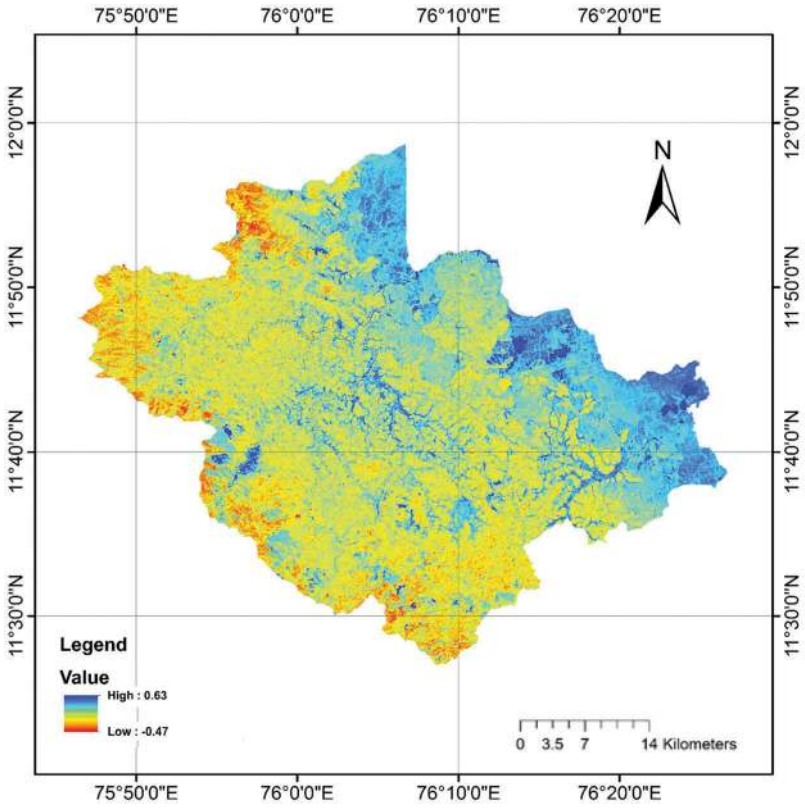

Figure 8. NDWI 2004.

various vegetation indices developed using Equations (5–12) are shown in Figures 10 and 11.

3.2 Land surface temperature

The ETM+ sensor carried on Landsat-7 satellite data is used to study for the LST of Wayanad district between 2004 and 2018. LST is defined as the skin-temperature of earth surface, which is detected by satellite imageries (Zhu, Lu, and Jia 2013). To estimate LST, the most widely used remote-sensing technique based on thermal band is used (Jimenez-Munoz 2003). Since the LISS-III sensor is not having any thermal band, LST analysis using LISS-III satellite imagery is not possible. Hence, Thermal band (Band 6) of ETM+ sensor having wavelength 10.40–12.50 µm acquired both low and high gain data at 60 m resolution. These images are resampled into 30 m resolution using spline interpolation and then used in this study. The low-gain data is used when surface brightness is higher, while high-gain data is used if the surface brightness is lower. Image saturation is comparatively better for low-gain data. Moderate Resolution Imaging Spectro-radiometer (MODIS) sensor carried on Aqua and Terra satellites also have thermal bands (Bands 31 and 32), but resolution of both MODIS and LISS-III sensors is beyond comparison. Hence, we choose low-gain thermal band of ETM+ sensor carried on Landsat-7 with spatial resolution 30 m for the LST estimation.

4. Discussions

4.1 LST vs. NDVI

Vegetative lands absorb an adequate amount of heat through transpiration and release low radiations leading to decrease in surface radiant temperatures. The modifications in topography of the area and its surface type exhibited noticeable difference in the LST. Discernibly high temperatures are observed during summer season due to changes in land-use characteristics of the area from 2004 to 2018. The mean surface temperature of the study area classified under paddy field dropped from 27.43 to 25.52°C during 2004–2018 periods. Paddy field classification shows the highest surface temperature among all other vegetation classifications. Since several paddy fields are converted into banana, ginger, tapioca and yam cultivations, certain region shows a rise in surface temperature of nearly 2.5°C. During paddy cultivation, water can stay on the land. Thus, conversion of paddy field to crop cultivation land reduces the moisture content of soil, which in turn increases the LST of those

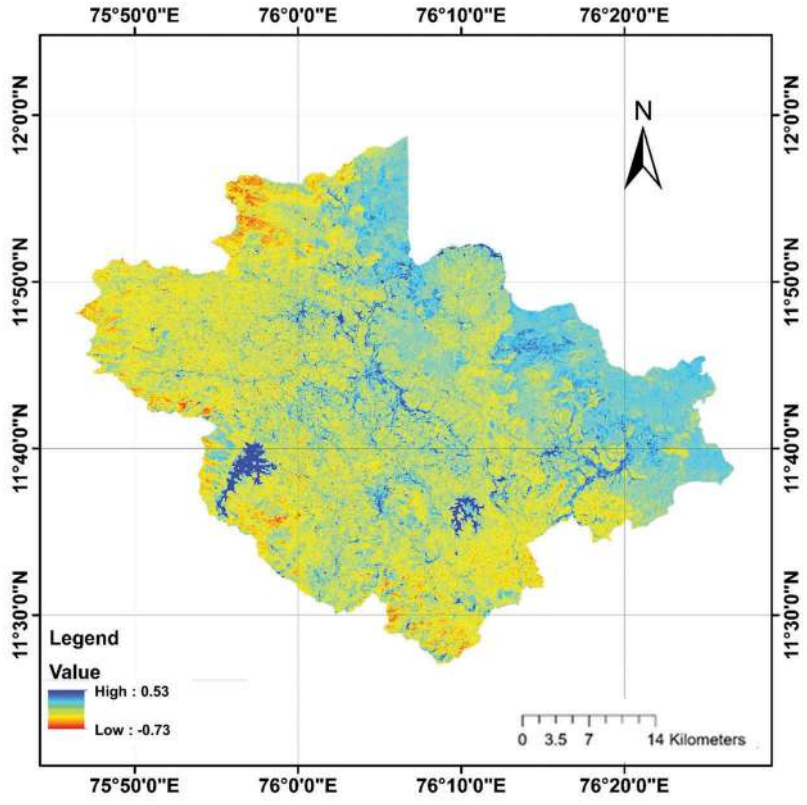

Figure 9. NDWI 2018.

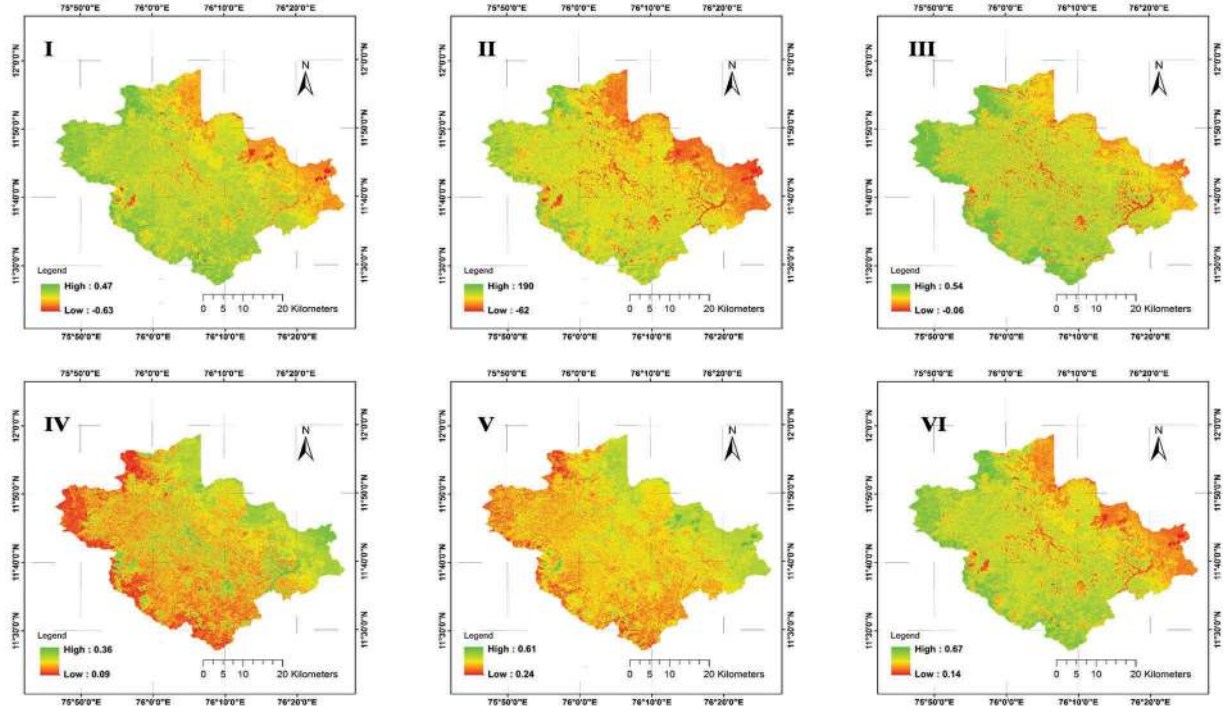

Figure 10. Vegetative indices of 2004 GNDVI, DVI, VI green, NR, NG and NNIR.

areas. Overall, this classification shows lower surface temperature pattern in 2018 then 2004. Mean LST in whole forest area decreased from 26.98 to 22.50°C during 2004 and 2018. Observations show that the LST scale at forest range near Tholpetty region (North-East) is decreased from 22.92 to 19.78°C. However, the LST in

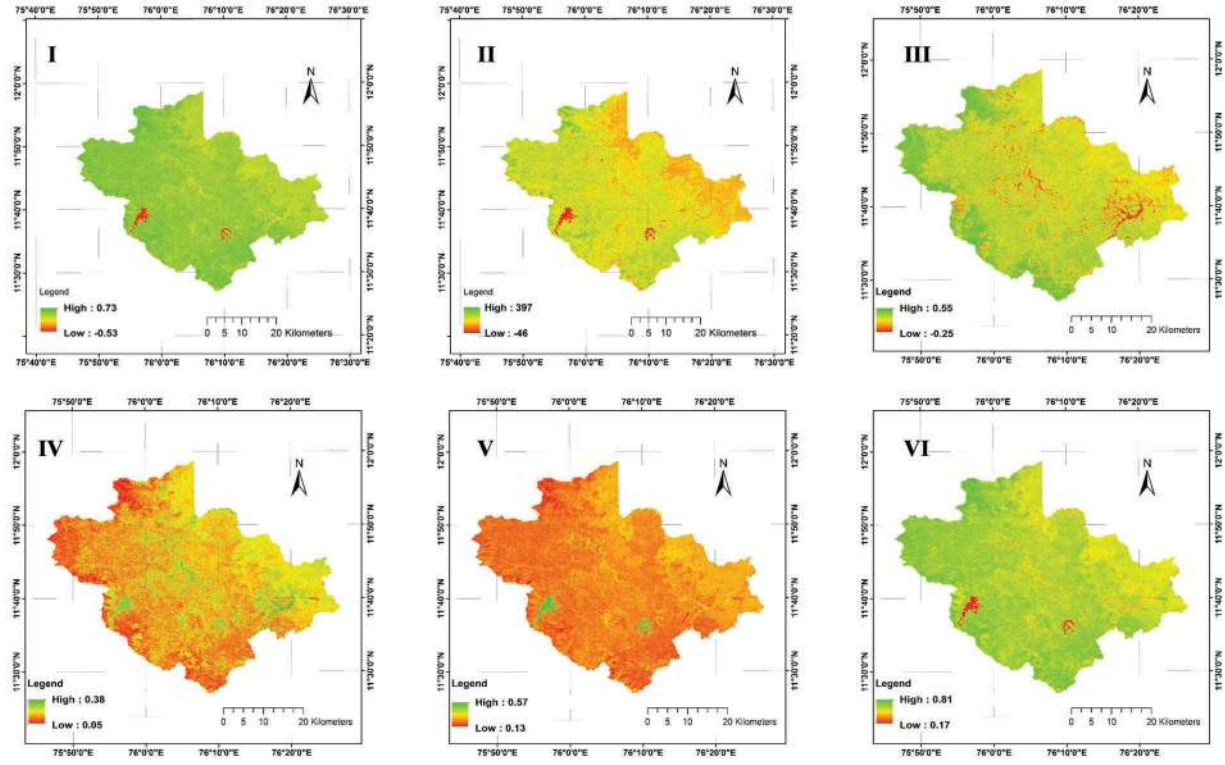

Figure 11. Vegetative indices of 2018 GNDVI, DVI, VI green, NR, NG and NNIR.

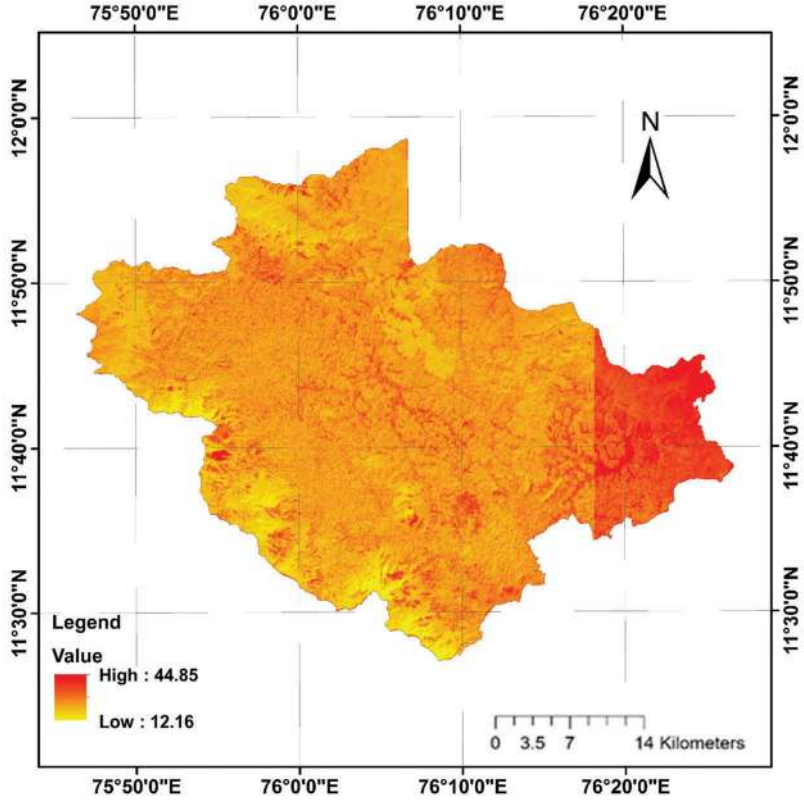

Figure 12. LST map of Wayanad 2004.

Muthanga wildlife sanctuary shows LST of 29.38 and 24.07°C during 2004 and 2018, respectively. Vast areas of bamboo have undergone degradation in the forest and wildlife protected zones of the Wayanad district during 2008 to 2013. Negative correlation was observed in the spatial distribution of NDVI and LST patterns after water body removal.

4.2 Analysis of surface temperature difference with LULC

Overall, in this study surface temperature scale shows decreasing trend during 2004 and 2018 in Wayanad district, i.e. LST value during 2018 shows surface temperature of 22.28°C which is comparatively lower than surface temperature 24.01°C of 2004. The spatial variation in LST of 2004 and 2018 of study area is shown in Figures 12 and 13. In water body classified area, the surface temperature decreased by nearly 4.5°C. The mean LST during 2004 and 2018 is 24.2 and 20.3°C, respectively. The locations of reservoirs in the study area also show a decrease of 6.45°C during the study period, i.e. 27.25 (in 2004) and 20.79°C (in 2018). The land cover exists as agricultural crops and paddy field during the year 2004, since the Banasurasagar and Karappuzha dams were not commissioned up to the year 2004. This area was converted into dam catchment area later and this might have led to decrease in surface temperature of the area.

One of the distinct factors is that the lowest LST among all LULC classifications is observed in dense classification during 2004 and 2018. Overall, the LST scale of densely vegetated areas dropped from 20.5 to 19.1°C in Wayanad district during 2004 and 2018, respectively. The dense vegetated areas adjacent to Chembra peak (South) and Periya forest (North-West) revealed almost similar surface temperature, i.e. around 18.6 and 21.7°C, respectively, for the years 2004 and 2018. However, surface temperature at both densely vegetated regions like Brahmagiri hills (North) and Banasura hills (South) shows a fall from 21.2 to 18.3°C during 2018.

In agricultural areas, an increase of 1.7°C is observed over the study area during 2004 and 2018, i.e. the LST value estimated in 2004 is 23.9°C and 2018 is 22.5°C. Here, agricultural crops are characterized based on the nearby municipal settlements in study area. The agricultural LULC classified areas around Kalpetta (11.6103° N, 76.0828° E) and Sulthan Bathery (11.6656° N, 76.2627° E) region shows an average difference of 1.1°C, i.e. 24.6 to 23.5°C.

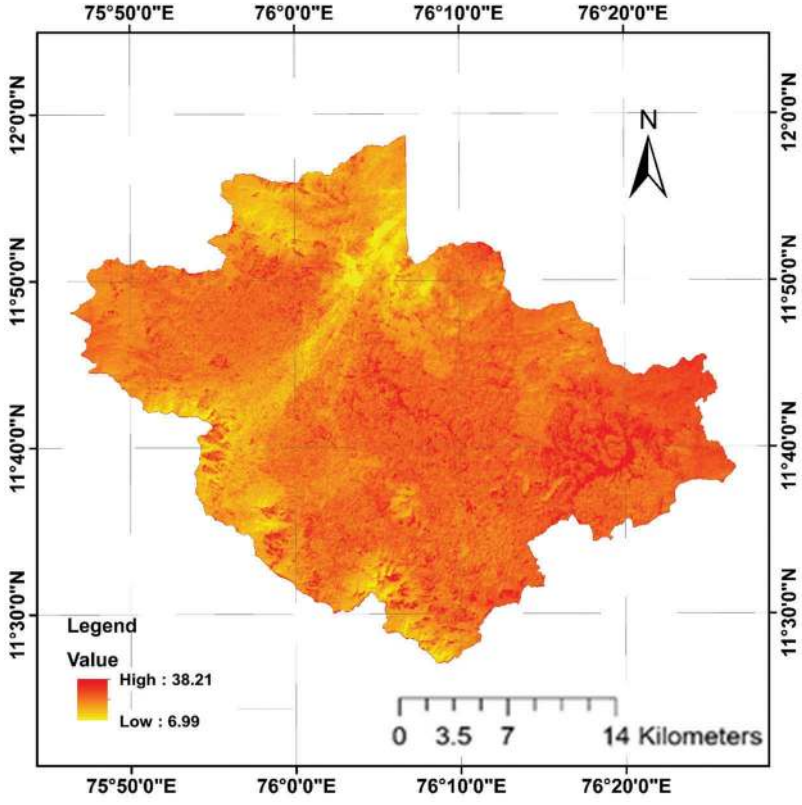

Figure 13. LST map of Wayanad 2018.

However, a variation of 3.0°C can be observed in Mananthavady (11.8014°N, 76.0044°E) region (surface temperature is dropped from 23.9°C to 20.8°C). We have detected the similar variation of dense classification vs other classes in Mananthavady region. But a unique LST trend is noticed in and around Meenangadi (11.6596°N, 76.1726°E) panchayath region which shows almost an equal surface temperature value of 23.8°C in both 2004 and 2018. Meenangadi panchayath in Wayanad district is currently on a mission towards world's first carbon neutral panchayath by 2020 (Nagar and Kawdiar 2018).

Overall, 0.5°C rise in built-up surface temperature is experienced during the study period in Wayanad. Urban settlements in the study area like Kalpetta and Mananthavady show a decrease of 0.66°C in LST, while all other urban built-ups and rural built-ups show an increasing trend of approximately 1°C whereas temperature of rural town areas has a rise of 1.19°C. Hence, urban development in the study area and LULC classification in correspondence with LST variation carry up radiation from surface types like gravels, metallic and concrete. In Wayanad, rural towns are more developing rather than urban townships. The rural settlements show an average surface temperature increase of 0.29°C in the year 2018, i.e. an average of 24.97 and 25.26°C during 2004 and 2018, respectively. An increase of nearly 3.2°C in LST is noted at stone mining quarries in various locations of the district. Conversion of agricultural crops to rocky areas for the mining activities lead to increase of surface temperature from 24.7 to nearly 27.9°C. Similar to the study area, the other parts of Kerala viz., Kuttanand (Singh 2018), Alappuzha (Prasad and Ramesh 2019), Thiruvananthapuram (Arulbalaji and Maya 2019), Bharathapuzha basin (Raj, Azeez, and Use 2010), etc., have shown a prominent surge towards urbanization from the period of 2004–2014. Further, the increase in vegetative land and decrease in LST is observed due to varied agricultural practices. However, the studies on sprawling in urban core cities indicate the increasing LST values of surrounding dense built-up region (Shastri and Ghosh 2019). LULC classification and changes in temperatures due to increasing urbanization are also studied in other parts of India (Chennai (Amirtham and Devadas 2009),(David Sundersingh 1990; Devadas and Rose 2009), Delhi (Mallick, Kant, and Bharath 2008; Mohan et al. 2012; Kikon et al. 2016), Pune (Deosthali 2000), Hyderabad (Sundara Kumar, Udaya Bhaskar, and Padma Kumari 2017; Badarinath et al. 2005), Mumbai (Lei et al. 2008; Grover and Singh 2015), Bangalore (Ramachandra, Bharath, and Gupta 2018), Ahmedabad (Vyas, Shastri, and Joshi 2014), Lucknow (Singh, Kikon, and Verma 2017), Jaipur (Jalan and Sharma 2014; Chandra, Sharma, and Dubey 2018), Surat (Sharma, Ghosh, and Joshi 2013), Kochi (Thomas et al. 2014) and Nagpur (Agarwal, Sharma, and Taxak 2014)), producing a similar negative correlation in case of vegetative features vs. LST and positive in case of non-evaporating surfaces vs. temperature.

5. Conclusion

The temporal changes in LULC and LST in Wayanad, a district of Kerala from southern India during 2004 and 2018, are analysed in the present study. After the analysis, it is evident that overall vegetation cover increased to a certain extent in the study area from 2004 to 2018. Major LULC changes are observed in the water body and built-up classes. The increase in water body classification during 2018 is mainly due to the commissioning of two dams in the Wayanad during the mid of year 2004, i.e. after the capture of 2004 image used for this study. These changes can be directly or indirectly linked to human intervention and population growth. The infrastructural or other developmental activities due to human intervention in Wayanad district seriously depleted agricultural cultivatable land area. Along with the human intervention into agricultural crops, the paddy field near developing zones are also getting transformed into built-ups. This conversion process grabs the moisture content in topmost soil surface layer. It is clear from the LULC map of 2004 and 2018 that the built-up areas' developmental activities are occurring in rural areas rather than urban areas during 2018.

The LST analysis results from the overall study area show a decreasing pattern between the years 2004 and 2018. LST in paddy classified area shows the highest surface temperature among the vegetation classes. Conversion of paddy field into other agricultural cultivating land and barren lands increases surface temperature scale nearly 2.5°C. The increase in LST after conversion of paddy field is due to loss of moisture from surface soil. Dense shows lowest LST scale among the classes which ranges from 20.5 to 19.1°C. However, there is an increase in surface temperature of 1°C as observed over the built-up areas. Rural built-ups show an increased temperature range than urban built-ups. Overall, the vegetation has increased in certain areas. This is accompanied by a decrease in surface temperature of nearly 2°C in the study area. This is contradictory to what is expected, since there is also an increase in built-up areas associated with increased temperature of approximately

0.5°C. On taking Wayanad, there is an increase in vegetation associated with decrease in surface temperature.

Acknowledgements

The authors are thankful to NRSC, Hyderabad, and USGS, United States, for providing satellite imageries for this study. We are also thankful to Dr. Babou. C, Scientist (Agronomy), Regional Coffee Research Station, Wayanad, for supplying meteorological data of study area. We are also grateful to Nansen Environmental Research Centre (India), Kochi, for providing facilities to carry out the study.

Disclosure Statement

No potential conflict of interest was reported by the authors.

ORCID

B. Srimuruganandam http://orcid.org/0000-0003-1324-5552
Abhinav Wadhwa http://orcid.org/0000-0003-4982-3270

References

Achmad, A., S. Hasyim, B. Dahlan, and D. N. Aulia. 2015. "Modeling of Urban Growth in Tsunami-prone City Using Logistic Regression: Analysis of Banda Aceh, Indonesia." *Applied Geography* 62: 237–246. doi:10.1016/j.apgeog.2015.05.001.

Agarwal, R., U. Sharma, and A. Taxak. 2014. "Remote Sensing Based Assessment of Urban Heat Island Phenomenon in Nagpur Metropolitan Area." *International Journal of Information and Computer Technology* 4: 1069–1074.

Amirtham, L. R., and M. Devadas. 2009. "Analysis of Land Surface Temperature and Land Use/Land Cover Types Using Remote Sensing Imagery - a Case in Chennai." In *The Seventh International Conference on Urban Climate*. Yokohama, Japan, pp. 1–4.

Anderson, K., E. Houk, S. Mehl, and D. L. Brown. 2017. "The Modeled Effects of Rice Field Idling on Groundwater Storage in California's Sacramento Valley." *Journal of Water Resource and Protection* 09: 786–798. doi:10.4236/jwarp.2017.97052.

Antherjanam, G., S. Chandrakaran, and S. Adarsh. 2010. "Landslide Hazards Zonation Incorporating Geotechnical Characteristics: A Case Study of Wayanad District in Kerala." In *Indian Geotechnical Conference.* IIT Bombay, Mumbai, pp. 655–658.

Aronica, G. T., and L. G. Lanza. 2005. "Drainage Efficiency in Urban Areas: A Case Study." *Hydrological Processes* 19: 1105–1119. doi:10.1002/()1099-1085.

Arulbalaji, P., and K. Maya. 2019. "Effects of Land Use Dynamics on Hydrological Response of Watershed: A Case Study of Chittar Watershed, Vamanapuram River Basin, Thiruvananthapuram District, Kerala, India." *Water Conservation Science and Engineering* 4: 33–41. doi:10.1007/s41101-019-00066-5.

Atkinson, P. M., and P. Lewis. 2000. "Geostatistical Classification for Remote Sensing: An Introduction." *Computers & Geosciences* 26: 361–371. doi:10.1016/S0098-3004(99)00117-X.

Badarinath, K. V. S., T. R. Kiran Chand, K. Madhavi Latha, and V. Raghavaswamy. 2005. "Studies on Urban Heat Islands Using ENVISAT AATSR Data." *Journal of the Indian Society of Remote Sensing* 33: 495–501. doi:10.1007/BF02990734.

Blanzieri, E., and F. Melgani. 2008. "Nearest Neighbor Classification of Remote Sensing Images with the Maximal Margin Principle." *IEEE Transactions on Geoscience and Remote Sensing* 46: 1804–1811. doi:10.1109/TGRS.2008.916090.

Buschmann, C., and E. Nagel. 1993. "In Vivo Spectroscopy and Internal Optics of Leaves as Basis for Remote Sensing of Vegetation." *International Journal of Remote Sensing* 14: 711–722. doi:10.1080/01431169308904370.

Cai, G., M. Du, and Y. Xue. 2011. "Monitoring of Urban Heat Island Effect in Beijing Combining ASTER and TM Data." *International Journal of Remote Sensing* 32: 1213–1232. doi:10.1080/01431160903469079.

Cammerer, H., A. H. Thieken, and P. H. Verburg. 2013. "Spatio-temporal Dynamics in the Flood Exposure Due to Land Use Changes in the Alpine Lech Valley in Tyrol (Austria)." *Natural Hazards* 68: 1243–1270. doi:10.1007/s11069-012-0280-8.

Chandra, S., D. Sharma, and S. K. Dubey. 2018. "Linkage of Urban Expansion and Land Surface Temperature Using Geospatial Techniques for Jaipur City, India." *Arabian Journal of Geosciences* 11: 1-9.

Dale, V. H., B. D. Santer, T. M. L. Wigley, J. S. Boyle, D. J. Gaffen, J. J. Hnilo, D. Nychka, et al. 1997. "Statistical Significance of Trends and Trend Differences in Layer-average Atmospheric Temperature Time Series." *Journal of Geophysical Research* 105: 7337–7356.

David Sundersingh, S. 1990. "Effect of Heat Islands over Urban Madras and Measures for Its Mitigation." *Energy and Buildings* 15: 245–252. doi:10.1016/0378-7788(90)90136-7.

Deep, S., and A. Saklani. 2014. "Urban Sprawl Modeling Using Cellular Automata." *Egyptian Journal of Remote Sensing and Space Sciences* 17: 179–187.

Deer, P. J., and P. Eklund. 2003. "A Study of Parameter Values for A Mahalanobis Distance Fuzzy Classifier." *Fuzzy Sets and Systems* 137: 191–213. doi:10.1016/S0165-0114(02)00220-8.

Deosthali, V. 2000. "Impact of Rapid Urban Growth on Heat and Moisture Islands in Pune City, India." *Atmospheric Environment* 34: 2745–2754. doi:10.1016/S1352-2310(99)00370-2.

Devadas, M. D., and A. L. Rose. 2009. "Urban Factors and the Intensity of Heat Island in the City of Chennai." In *Seventh Int. Conf. Urban Clim*. 29 June - 3 July 2009, 3–6. Yokohama, Japan.

Dhodhi, M. K., J. A. Saghri, I. Ahmad, and R. Ul-Mustafa. 1999. "D-ISODATA: A Distributed Algorithm for Unsupervised Classification of Remotely Sensed Data on Network of Workstations." *Journal of Parallel and Distributed Computing* 59: 280–301. doi:10.1006/jpdc.1999.1573.

Dubovyk, O., R. Sliuzas, and J. Flacke. 2011. "Spatio-temporal Modelling of Informal Settlement Development in Sancaktepe District, Istanbul, Turkey." *ISPRS Journal of Photogrammetry and Remote Sensing* 66: 235–246. doi:10.1016/j.isprsjprs.2010.10.002.

Dwivedi, R. S., K. Sreenivas, and K. V. Ramana. 2005. "Land-use/land-cover Change Analysis in Part of Ethiopia Using Landsat Thematic Mapper Data." *International Journal of Remote Sensing* 26: 1285–1287. doi:10.1080/01431160512331337763.

Fan, F., Q. Weng, and Y. Wang. 2007. "Land Use and Land Cover Change in Guangzhou, China, from 1998 to 2003, Based on

Landsat TM/ETM+ Imagery." *Sensors* 7: 1323–1342. doi:10.3390/s7071323.

Fleiss, J. L., J. Cohen, and B. S. Everitt. 1969. "Large Sample Standard Errors of Kappa and Weighted Kappa." *Psychological Bulletin* 72: 323–327. doi:10.1037/h0028106.

Flint, R. 1994. *Historic Land Use and Carbon Estimates for South and South East Asia 1880–1980*. 420. doi:10.3168/jds.S0022-0302(94)77044-2.

Foody, G. M. 2002. "Status of Land Cover Classification Accuracy Assessment." *Remote Sensing of Environment* 80: 185–201. doi:10.1016/S0034-4257(01)00295-4.

Friedl, M. A., and C. E. Brodley. 1997. "Decision Tree Classification of Land Cover from Remotely Sensed Data." *Remote Sensing of Environment* 61: 399–409. doi:10.1016/S0034-4257(97)00049-7.

Gislason, P. O., J. A. Benediktsson, and J. R. Sveinsson. 2006. "Random Forests for Land Cover Classification." *Pattern Recognition Letters* 27: 294–300. doi:10.1016/j.patrec.2005.08.011.

Gitelson, A. A., Y. J. Kaufman, R. Stark, and D. Rundquist. 2002. "Novel Algorithms for Remote Estimation of Vegetation Fraction." *Remote Sensing of Environment* 80: 76–87. doi:10.1016/S0034-4257(01)00289-9.

Grover, A., and R. Singh. 2015. "Analysis of Urban Heat Island (UHI) in Relation to Normalized Difference Vegetation Index (NDVI): A Comparative Study of Delhi and Mumbai." *Environments* 2: 125–138. doi:10.3390/environments2020125.

Huang, C., L. S. Davis, and J. R. G. Townshend. 2002. "International Journal of Remote Sensing an Assessment of Support Vector Machines for Land Cover Classification an Assessment of Support Vector Machines for Land Cover Classi Cation." *International Journal of Remote Sensing* 23: 725–749. doi:10.1080/01431160110040323.

Jalan, S., and K. Sharma. 2014. "Spatio-temporal Assessment of Land Use/land Cover Dynamics and Urban Heat Island of Jaipur City Using Satellite Data." *ISPRS - International Archives of the Photogrammetry, Remote Sensing and Spatial Information Sciences* XL–8: 767–772. doi:10.5194/isprsarchives-XL-8-767-2014.

Jha, C. S., C. B. S. Dutt, and K. S. Bawa. 2000. "Deforestation and Land Use Changes in Western Ghats, India." *Current Science* 79: 231–238.

Jiang, H., D. Zhao, Y. Cai, and S. An. 2012. "A Method for Application of Classification Tree Models to Map Aquatic Vegetation Using Remotely Sensed Images from Different Sensors and Dates." *Sensors (Switzerland)* 12: 12437–12454. doi:10.3390/s120912437.

Jimenez-Munoz, J. C. 2003. "Land Surface Temperature Retrieval from CBERS-02 IRMSS Thermal Infrared Data and Its Applications in Quantitative Analysis of Urban Heat Island Effect." *Journal of Geophysical Research* 108: 4688.

Kavzoglu, T., and P. M. Mather. 2003. "The Use of Backpropagating Artificial Neural Networks in Land Cover Classification." *International Journal of Remote Sensing* 24: 4907–4938. doi:10.1080/0143116031000114851.

Khan, M. M. H., I. Bryceson, K. N. Kolivras, F. Faruque, M. M. Rahman, and U. Haque. 2014. "Natural Disasters and Land-use/land-cover Change in the Southwest Coastal Areas of Bangladesh." *Regional Environmental Change* 15: 241–250. doi:10.1007/s10113-014-0642-8.

Kikon, N., P. Singh, S. K. Singh, and A. Vyas. 2016. "Assessment of Urban Heat Islands (UHI) of Noida City, India Using Multi-temporal Satellite Data." *Sustainable Cities and Society* 22: 19–28. doi:10.1016/j.scs.2016.01.005.

Kuriakose, S. L., G. Sankar, and C. Muraleedharan. 2009. "History of Landslide Susceptibility and a Chorology of Landslide-prone Areas in the Western Ghats of Kerala, India." *Environmental Geology* 57: 1553–1568. doi:10.1007/s00254-008-1431-9.

Lambin, E. F., H. J. Geist, and E. Lepers. 2003. "Dynamics of Land-Use and Land-Cover Change in Tropical Regions." *Annual Review of Environment and Resources* 28: 205–241. doi:10.1146/annurev.energy.28.050302.105459.

Lei, M., D. Niyogi, C. Kishtawal, R. A. Pielke, A. Beltrán-Przekurat, T. E. Nobis, and S. S. Vaidya. 2008. "Effect of Explicit Urban Land Surface Representation on the Simulation of the 26 July 2005 Heavy Rain Event over Mumbai, India." *Atmospheric Chemistry and Physics* 8: 5975–5995. doi:10.5194/acp-8-5975-2008.

Li, M., S. Zang, B. Zhang, S. Li, and C. Wu. 2014. "A Review of Remote Sensing Image Classification Techniques: The Role of Spatio-contextual Information." *European Journal of Remote Sensing* 47: 389–411. doi:10.5721/EuJRS20144723.

Li, X., W. Zhou, and Z. Ouyang. 2013. "Forty Years of Urban Expansion in Beijing: What Is the Relative Importance of Physical, Socioeconomic, and Neighborhood Factors?" *Applied Geography* 38: 1–10. doi:10.1016/j.apgeog.2012.11.004.

Lo, C. P., and J. Choi. 2004. "A Hybrid Approach to Urban Land Use/cover Mapping Using Landsat 7 Enhanced Thematic Mapper Plus (ETM +) Images." *International Journal of Remote Sensing* 25: 2687–2700. doi:10.1080/01431160310001618428.

Loibl, W., and T. Toetzer. 2003. "Modeling Growth and Densification Processes in Suburban Regions - Simulation of Landscape Transition with Spatial Agents." *Environmental Modelling & Software* 18: 553–563. doi:10.1016/S1364-8152(03)00030-6.

Mallick, J., Y. Kant, and B. Bharath. 2008. "Estimation of Land Surface Temperature over Delhi Using Landsat-7 ETM+." *Journal of Indian Geophysical Union* 12: 131–140.

Marconcini, M., G. Camps-Valls, and L. Bruzzone. 2009. "A Composite Semisupervised SVM for Classification of Hyperspectral Images." *IEEE Geoscience and Remote Sensing Letters* 6: 234–238. doi:10.1109/LGRS.2008.2009324.

Mas, J.-F., A. Velázquez, J. R. Díaz-Gallegos, R. Mayorga-Saucedo, C. Alcántara, G. Bocco, R. Castro, T. Fernández, and A. Pérez-Vega. 2004. "Assessing Land Use/cover Changes: A Nationwide Multidate Spatial Database for Mexico." *International Journal of Applied Earth Observation and Geoinformation* 5: 249–261. doi:10.1016/j.jag.2004.06.002.

Mather, P. M., and M. Koch. 2010. *Computer Processing of Remotely-Sensed Images: An Introduction*. 4th ed. ISBN 9780470742389. Wiley-Blackwell

McFeeters, S. K. 1996. "The Use of the Normalized Difference Water Index (NDWI) in the Delineation of Open Water Features." *International Journal of Remote Sensing* 17: 1425–1432. doi:10.1080/01431169608948714.

McIver, D. K., and M. A. Friedl. 2002. "Using Prior Probabilities in Decision-tree Classification of Remotely Sensed Data." *Remote Sensing of Environment* 81: 253–261. doi:10.1016/S0034-4257(02)00003-2.

Mohan, M., Y. Kikegawa, B. R. Gurjar, S. Bhati, A. Kandya, and K. Ogawa. 2012. "Urban Heat Island Assessment for a Tropical

Urban Airshed in India." *Atmospheric Climate Science* 02: 127–138.
Morisette, J. T., and S. Khorram. 2000. "Accuracy Assessment Curves for Satellite-based Change Detection." *Photogrammetric Engineering and Remote Sensing* 66: 875–880.
Mustafa, A., A. Heppenstall, H. Omrani, I. Saadi, M. Cools, and J. Teller. 2018. "Modelling Built-up Expansion and Densification with Multinomial Logistic Regression, Cellular Automata and Genetic Algorithm." *Computers, Environment and Urban Systems* 67: 147–156. doi:10.1016/j.compenvurbsys.2017.09.009.
Nagar, J., and P. O. Kawdiar. 2018. *Carbon Neutral Meenangadi – Assessment and Recommendations*.
Pal, M., and P. M. Mather. 2005. "Support Vector Machines for Classification in Remote Sensing." *International Journal of Remote Sensing* 26: 1007–1011. doi:10.1080/01431160512331314083.
Pal, S., and O. Akoma. 2009. "Water Scarcity in Wetland Area within Kandi Block of West Bengal: A Hydro-Ecological Assessment." *Ethiopian Journal of Environmental Studies and Management* 2. doi:10.4314/ejesm.v2i3.48260..
Prasad, G., and M. V. Ramesh. 2019. "Spatio-Temporal Analysis of Land Use/Land Cover Changes in an Ecologically Fragile Area—Alappuzha District, Southern Kerala, India." *Natural Resources Research* 28: 31–42. doi:10.1007/s11053-018-9419-y.
Prenzel, B. 2004. "Remote Sensing-based Quantification of Land-cover and Land-use Change for Planning." *Progress in Planning* 61: 281–299. doi:10.1016/S0305-9006(03)00065-5.
Raj, P. P. N., P. A. Azeez, and L. Use. 2010. "Land Cover Changes in A Tropical River Basin: A Case from Bharathapuzha River Basin, Southern India." *Journal of Geographic Information System* 02: 185–193.
Ramachandra, T. V., S. Bharath, and N. Gupta. 2018. "Modelling Landscape Dynamics with LST in Protected Areas of Western Ghats, Karnataka." *Journal of Environmental Management* 206: 1253–1262. doi:10.1016/j.jenvman.2017.08.001.
Reis, S. 2008. "Analyzing Land Use/land Cover Changes Using Remote Sensing and GIS in Rize, North-East Turkey." *Sensors* 8: 6188–6202. doi:10.3390/s8106188.
Rimal, B., R. Sharma, R. Kunwar, H. Keshtkar, N. E. Stork, S. Rijal, S. A. Rahman, and H. Baral. 2019. "Effects of Land Use and Land Cover Change on Ecosystem Services in the Koshi River Basin, Eastern Nepal." *Ecosystem Services* 38: 100963. doi:10.1016/j.ecoser.2019.100963.
Rollet, R., G. B. Benie, W. Li, S. Wang, and J. M. Boucher. 1998. "Image Classification Algorithm Based on the RBF Neural Network and K-means." *International Journal of Remote Sensing* 19: 3003–3009. doi:10.1080/014311698214398.
Russell, G., and K. G. Congalton. 2013. *Assessing the Accuracy of Remotely Sensed Data*. Vol. 53. ISBN 9788578110796.
Sagan, C., O. B. Toon, and J. B. Pollack. 1979. "Anthropogenic Albedo Changes and the Earth's Climate." *Science (80-)* 206: 1363–1368. doi:10.1126/science.206.4425.1363.
Sand, E. R. 2016. *Government of Kerala District Survey Report*.
Schneider, A. 2012. "Remote Sensing of Environment Monitoring Land Cover Change in Urban and Peri-urban Areas Using Dense Time Stacks of Landsat Satellite Data and a Data Mining Approach." *Remote Sensing of Environment* 124: 689–704. doi:10.1016/j.rse.2012.06.006.
Settle, J. J., and S. A. Briggs. 1987. "Fast Maximum Likelihood Classification of Remotely-sensed Imagery." *International Journal of Remote Sensing* 8: 723–734. doi:10.1080/01431168708948683.
Shalaby, A., and R. Tateishi. 2007. "Remote Sensing and GIS for Mapping and Monitoring Land Cover and Land-use Changes in the Northwestern Coastal Zone of Egypt." *Applied Geography* 27: 28–41. doi:10.1016/j.apgeog.2006.09.004.
Sharma, R., A. Ghosh, and P. K. Joshi. 2013. "Spatio-temporal Footprints of Urbanisation in Surat, the Diamond City of India (1990–2009)." *Environmental Monitoring and Assessment* 185: 3313–3325. doi:10.1007/s10661-012-2792-9.
Shastri, H., and S. Ghosh. 2019. "Urbanisation and Surface Urban Heat Island Intensity (SUHII)." *Climate Change Signals Response* 73–90. http://link.springer.com/10.1007/978-981-13-0280-0_5
Singh, C. K. 2018. *Geospatial Applications for Natural Resources Management*. CRC Press. ISBN 9781138626287. Broken Sound Parkway NW, London, New York.
Singh, P., N. Kikon, and P. Verma. 2017. "Impact of Land Use Change and Urbanization on Urban Heat Island in Lucknow City, Central India." *Sustainable Cities and Society* 32: 100–114. doi:10.1016/j.scs.2017.02.018.
Song, J., S. Du, X. Feng, and L. Guo. 2014. "The Relationships between Landscape Compositions and Land Surface Temperature: Quantifying Their Resolution Sensitivity with Spatial Regression Models." *Landscape and Urban Planning* 123: 145–157. doi:10.1016/j.landurbplan.2013.11.014.
Sripada, R. P., R. W. Heiniger, J. G. White, and A. D. Meijer. 2006. "Aerial Color Infrared Photography for Determining Early In-season Nitrogen Requirements in Corn." *Agronomy Journal* 98: 968–977. doi:10.2134/agronj2005.0200.
Sundara Kumar, K., P. Udaya Bhaskar, and K. Padma Kumari. 2017. "Assessment and Mapping of Urban Heat Island Using Field Data in the New Capital Region of Andhra Pradesh, India." *Indian Journal of Science and Technology* 10: 1–8. doi:10.17485/ijst/2017/v10i11/99983.
Thakkar, A. K., V. R. Desai, A. Patel, and M. B. Potdar. 2017. "Post-classification Corrections in Improving the Classification of Land Use/Land Cover of Arid Region Using RS and GIS: The Case of Arjuni Watershed, Gujarat, India." *Egyptian Journal of Remote Sensing and Space Sciences* 20: 79–89.
Thomas, G., A. P. Sherin, S. Ansar, and E. J. Zachariah. 2014. "Analysis of Urban Heat Island in Kochi, India, Using a Modified Local Climate Zone Classification." *Procedia Environmental Sciences* 21: 3–13. doi:10.1016/j.proenv.2014.09.002.
USGS *LANDSAT 7 (L7) DATA USERS HANDBOOK Version 1.0 June 2018*. 2018. Vol. 7.
Verma, A. K., P. K. Garg, K. S. H. Prasad, and V. K. Dadhwal. 2016. "Classification of LISS IV Imagery Using Decision Tree Methods." *ISPRS - International Archives of the Photogrammetry, Remote Sensing and Spatial Information Sciences* 41: 1061–1066. doi:10.5194/isprsarchives-XLI-B8-1061-2016.
Vyas, A., B. Shastri, and Y. Joshi. 2014. "Spatio-temporal Analysis of UHI Using Geo-spatial Techniques: A Case Study of Ahmedabad City." *ISPRS - International Archives of the Photogrammetry, Remote Sensing and Spatial Information Sciences* 40: 997–1002. doi:10.5194/isprsarchives-XL-8-997-2014.
Zhao, G. X., G. Lin, and T. Warner. 2004. "Using Thematic Mapper Data for Change Detection and Sustainable Use of Cultivated Land: A Case Study in the Yellow River Delta, China." *International Journal of Remote Sensing* 25: 2509–2522. doi:10.1080/01431160310001619571.
Zhu, W., A. Lu, and S. Jia. 2013. "Estimation of Daily Maximum and Minimum Air Temperature Using MODIS Land Surface Temperature Products." *Remote Sensing of Environment* 130: 62–73. doi:10.1016/j.rse.2012.10.034.